ELSEVIER

Applied Catalysis A: General 199 (2000) 263–273

APPLIED CATALYSIS A: GENERAL

www.elsevier.com/locate/apcata

Deactivation of Ni–Mo/Al_2O_3 catalysts aged in a commercial reactor during the hydrotreating of deasphalted vacuum residuum

Manuel Nuñez Isaza [a,b], Zarith Pachon [a], Viatcheslav Kafarov [b], Daniel E. Resasco [c,*]

[a] *Ecopetrol-ICP (Colombian Petroleum Institute), Autopista Bucaramanga-Piedecuesta, Km 7, AA 4185, Bucaramanga, Colombia*

[b] *Universidad Industrial de Santander, Bucaramanga, Colombia*

[c] *School of Chemical Engineering and Materials Science, University of Oklahoma, 100 East Boyd St., Norman, OK 73019, USA*

Received 25 August 1999; received in revised form 13 December 1999; accepted 13 December 1999

Abstract

A series of Ni–Mo/Al_2O_3 catalysts for the hydrotreating of deasphalted vacuum bottoms has been investigated as fresh catalysts and after aging in an industrial reactor during a typical commercial run. Several structural parameters have been varied in the catalyst series. In particular, pore size, surface area, active metal loading and pellet size were changed to investigate the role of kinetic and diffusional phenomena present in this process. The samples were placed in different locations along the industrial reactor allowing for a comparative analysis of the different samples under varying environments, since along the reactor, quality, temperature, and H_2 partial pressure continuously change.

Fresh and aged samples were analyzed by a variety of techniques, which include atomic adsorption, scanning electron microscopy, X-ray microanalysis, BET, thermogravimetry and temperature-programmed oxidation. In addition, a laboratory trickle-bed reactor was used to compare the catalytic activity of fresh samples with the residual activity retained by the aged samples after the commercial run.

These catalysts deactivate by accumulation of metals and, to a lesser extent, coke deposition. These effects are governed by a competition of kinetic and diffusional phenomena. The kinetic phenomena, which involve adsorption and decomposition of metal-bearing compounds are mainly related to the active metal content and overall surface area of the catalyst, while the diffusion of the molecules inside the pellet are controlled by pore size distribution and pellet size. The current contribution shows how this type of comparative study can be used to identify the most appropriate catalyst configuration for a given set of reaction conditions and feedstock quality.

Keywords: Ni–Mo/Al_2O_3; Catalysts; Hydrotreatment; Vacuum residuum

1. Introduction

The continuous deterioration of the quality of crudes available to refineries, together with the drop in the fuel oil demand caused by environmental restrictions, have created a driving force for the development of more efficient technologies for the hydrotreating of residua, particularly vacuum bottoms. This bottom fraction comes from vacuum distillation units, which treat the heaviest fraction left in the residuum after the atmospheric distillation. The vacuum bottoms constitute a complex mixture of heavy compounds,

* Corresponding author. Tel.: +1-405-325-4370; fax: +1-405-325-5813.
E-mail address: resasco@ou.edu (D.E. Resasco)

0926-860X/00/$ – see front matter
PII: S0926-860X(00)00416-6

mainly resins and asphaltenes, with high molecular weight, low H/C ratio and high sulfur content. Asphaltenes are defined as the fraction that precipitates as a solid when the oil is treated in a solvent such as pentane. Resins can solubilize asphaltenes in the lighter fractions of oil via peptizing due to their properties, intermediate between the asphaltenes and the light fraction. A current strategy considered by refiners to add value to the vacuum bottoms is the hydrotreating of only the fraction that is cost-effective. This is done by removing the asphaltenes by solvent extraction, yielding a fraction rich in resins, which are less polar, less aromatic, with less sulfur, and with lower molecular weight than the asphaltenes. In addition, this fraction has a lower content of metals such as vanadium and nickel, which are normally present in crudes in the form of metalloporphyrins [1].

As these bottoms become heavier, the costs of residumm hydroprocessing necessarily increase due to the higher pressures required and the more rapid catalyst deactivation. These increased costs have in many cases prevented the implementation of these processes. The study of catalyst deactivation under industrial conditions and the effects of the different catalyst parameters on activity and stability may have an important impact on the selection of the most appropriate catalyst for these processes. In this contribution, we have investigated a series of alumina-supported Ni–Mo catalysts with varying porosity, pellet size, and Ni–Mo loading. These samples were aged under real industrial conditions by placing them in different locations inside the beds of two commercial hydrotreating reactors connected in series. After the aging process, the samples were characterized by several techniques to probe the phenomena that take place in different positions in the reactors.

2. Experimental

2.1. Catalyst samples investigated

Six different Ni–Mo/Al_2O_3 catalysts were investigated in the form of extrudates after aging in the industrial reactors. Some of the characteristics of the catalysts are summarized in Table 1. In this series, the average pore size ranged from 70 to 230 Å, the pellet size from 1 to 3 mm, and the metal content from 3 to 18 wt.% Mo, and from 1 to 2.3 wt.% Ni.

The samples were aged inside two fixed-bed industrial catalytic reactors with a catalyst load of approximately 40 tonnes each. The reactors, with processing capacity of 22 000 barrels per day, belong to the Ecopetrol refinery located in Barrancabermeja, Colombia. The process operated a LHSV of 1.0 h^{-1}, at a total pressure of 1500 psia and at a maximum temperature of 400°C. The length of the run was 241 days. To keep the production constant, the temperature was gradually increased as the catalyst deactivated. Therefore, during the 241-day run, the temperature at the inlet of the first reactor was increased from 330 to 355°C. At the same time, the temperature at the outlet of the second reactor went from 373°C at the beginning of the run to 395°C at the end of the run. Small samples of each catalyst were placed in metallic baskets, imbedded in two different locations inside the reactors: the top of the first reactor and the bottom of the second reactor. In all cases, the samples were placed in the central axis of the reactor. Furthermore, for two of the catalysts, A and D, additional samples were placed at intermediate locations inside the reactors. It can be considered that the samples located at the top of the first reactor were aged under conditions of the feed, that is deasphalted vacuum bottoms or demetallized oil (DMO). By contrast, the samples

Table 1
Characteristics of the catalysts investigated

	BET area (m^2/g)	Average pore size (Å)	Mo (%)	Ni (%)	Pellet size (mm)
A	320	126	8.1	2.3	1.03
B	266	98.6	10.5	1.5	3.1
C	264	136	3	1	1.0
D	146	233	8	2	2.1
E	173	82.8	12	2.3	1.55
F	329	71	18	1.8	1.3

Table 2
Quality of the feedstock and product

	DMO	DMOH
S (%)	1.3	0.3
Ni (ppm)	12.5	1.5
V (ppm)	14.5	2
Asphaltenes (ppm)	750	650

at the bottom of the second reactor were aged under conditions of the product, that is hydrotreated deasphalted vacuum bottoms or hydrotreated demetallized oil (HDMO). The quality of the feed and product of the hydrotreating reactors is summarized in Table 2.

2.2. Characterization of the aged samples

After the aging process inside the industrial reactors, the samples were characterized by atomic absorption and SEM/X-ray microanalysis in a Cambridge Instrument Stereoscan 240, equipped with EDAX detector CDU prime. The BET area and pore size distribution of aged samples was conducted in a Micromeritics ASAP 2000, after removal of the extractable hydrocarbons from the pellets, conducted in toluene for 48 h in a soxhlet apparatus, followed by treating in vacuum for 12 h. The hydrocarbon and coke deposits were analyzed by thermogravimetry in a Cahn 100 microbalance and by temperature-programmed oxidation, using a 4% O_2/He mixture and a temperature ramp of 9°C/min, using a mass spectrometer to detect the evolution of CO_2. In both cases, prior to the determination of coke deposits, the samples were heated to 540°C in He to eliminate the light hydrocarbons trapped in the pores of the catalyst.

To compare the activity of the fresh and aged samples, a laboratory reactor was employed. This continuous trickle-bed reactor, which held 120 cm^3 of catalyst, was operated isothermally at 350°C, at a pressure of 1500 psia, and at a space velocity LHSV of 2 h^{-1}. The reactor feed was deasphalted vacuum bottoms of Cano Limon crude oil.

3. Results

Table 3 summarizes the concentration of V and Ni retained on the different catalysts at the top of the first reactor, as measured by atomic absorption. Catalyst A, with a high surface area and relatively large pore size, exhibits the highest concentration of metals retained. Following this catalyst, samples C and D, also with large pores show a high metal retention capacity. By contrast, catalyst F, which has the smallest pore size shows very low concentration of metals. The distribution profiles of Ni and V through the catalyst pellet exhibited different shapes for each metal on the various catalysts. The profiles are illustrated in Fig. 1a–f for the different catalysts investigated. Catalysts A–D showed relatively homogeneous distributions of Ni, while catalysts E and F, which have the smallest pore sizes, showed inhomogeneities with accumulation of Ni near the external surface of the pellet. As discussed in the next section, this accumulation at the external surface is consistent with the low retention capacity exhibited by samples E and particularly F. The distribution of V is even more inhomogeneous. In this case, accumulation at the external surface occurs even on catalysts that have a high retention capacity. It is possible that at the beginning of the run the deposition is homogeneous, but later in the run, as the pores become narrower by the presence of metals and coke, deposition at the pore mouths becomes dominant.

Table 3
Concentration of V and Ni retained on the different catalysts at the top of the first reactor

	V (wt.%)	Ni (wt.%)	V/Ni ratio
$A_{(T)}$	26.1	22.6	1.15
$B_{(T)}$	15.2	14.6	1.04
$C_{(T)}$	18.4	12.6	1.46
$D_{(T)}$	17.9	14	1.28
$E_{(T)}$	14.1	12.7	1.1
$F_{(T)}$	4.2	4.6	0.9

The V/Ni ratio retained on the catalysts is also an interesting trend to analyze. For example, the deposition on catalysts A and D can be compared. These two catalysts both have large average pore sizes and the same initial metal content, but the pellet size of catalyst D is twice as large as that of catalyst A and its surface area significantly lower. Catalyst A retained more metals than catalyst D and it showed a large difference in the deposition profiles of Ni and V, while the distribution for catalyst D was almost identical for Ni and V.

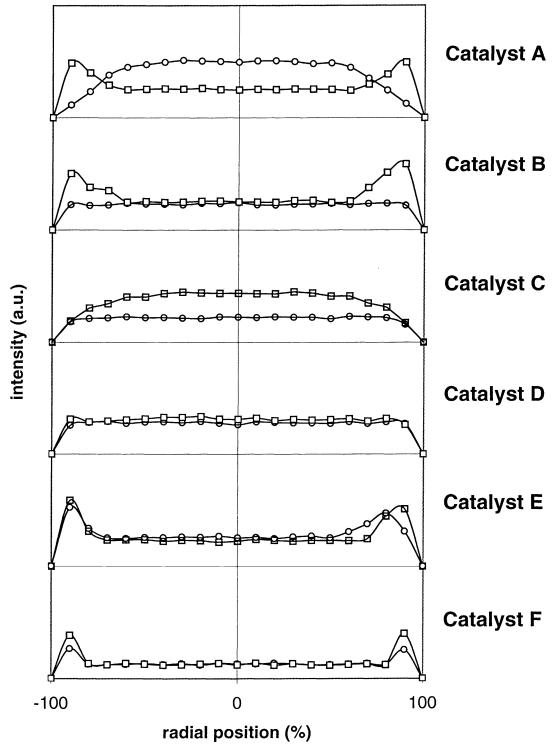

Fig. 1. Deposition profiles of Ni (circles) and V (squares) across the pellet for the different aged catalysts.

To further compare the behavior of these two catalysts, the variation of Ni, V and coke deposits as a function of position in the reactor bed for both the first and second reactor are shown in Figs. 2 and 3, respectively. It can be observed that catalyst A retained more metals than catalyst D in all points of the reactor. The majority of metals were retained in the first half of the first reactor. But, interestingly, the V/Ni ratio was kept constant throughout the two reactors for both catalysts. The carbon deposition greatly increased for catalyst A in the last half of the second reactor, showing that as the metal retention decreased the coke formation increased.

The quantification of the coke deposited at the top of the first reactor and at the bottom of the second are summarized in Table 4. The first column shows the weight loss observed on the samples after heating in He flow for 30 min at 540°C. The second column shows the weight loss observed on the same samples, previously heated and cooled in He, after

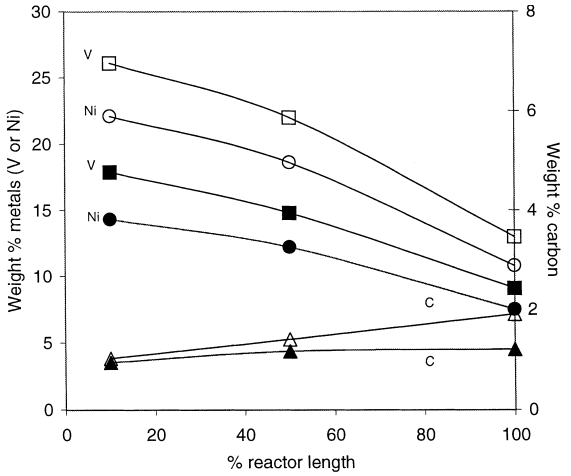

Fig. 2. Comparison of the deposition of metals and carbon along the length of the first reactor on two different catalysts. Open symbols are used for catalyst A, full symbols are used for catalyst D. Carbon (triangles), Ni (circles), and V (squares).

the subsequent heating in air up to 520°C. The last column shows the total carbon measurements determined by the LECCO method after the extraction in toluene described in Section 2. Interestingly, all samples corresponding to the top of the first reactor exhibited a low concentration of carbon deposits,

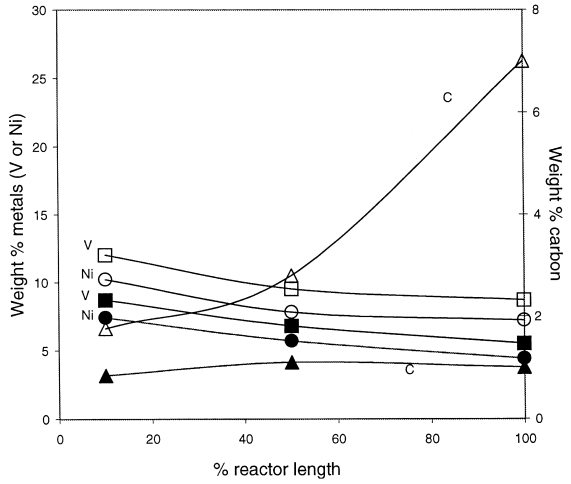

Fig. 3. Comparison of the deposition of metals and carbon along the length of the second reactor on two different catalysts. Open symbols are used for catalyst A, full symbols are used for catalyst D. Carbon (triangles), Ni (circles), and V (squares).

Table 4
Carbonaceous deposits (wt.%) left on the aged samples after the commercial run

	C eliminated by heating in He (520–540°C)	C oxidized in air (540°C) after pre-heating in He	LECCO analysis
$A_{(T)}$	2.7	1.2	2.9
$B_{(T)}$	3.7	3.8	5
$C_{(T)}$	2.8	1.0	2.7
$D_{(T)}$	3.1	1.4	3.3
$E_{(T)}$	2.4	1.9	3
$F_{(T)}$	2.9	1.3	3.1
$A_{(B)}$	5.4	10.4	7.9
$B_{(B)}$	0.9	12.3	8.1
$C_{(B)}$	2.1	10.7	7.7
$D_{(B)}$	11.9	1.3	7.9
$E_{(B)}$	2.4	11.4	8.1
$F_{(B)}$	4.1	11.2	7.7

contrasting with much higher carbon concentrations for all samples from the bottom of the second reactor. This difference may be due to the different operating conditions along the reactor, that is as one proceeds from the reactor inlet, the temperature increases and the hydrogen partial pressure decreases. As shown in Fig. 3 the greatest increase in coke formation would occur in the last part of the second reactor. Contrarily to the case of metal retention capacities, which were significantly lower for the small-pore samples, the carbon deposition did not vary within the catalyst series. Only sample D showed a somewhat peculiar behavior. Even though the overall amount of carbon on this sample as determined by LECCO was about the same as that on the other samples, the determination conducted by thermogravimetry indicated that most of the carbonaceous deposits were eliminated by heating at 540°C in an inert atmosphere.

Fig. 4 shows the TPO profiles for the various samples taken from the bottom of the second reactor. It can be seen that, although this is the part of the reactor with the greatest formation of coke, most of the coke for all the samples can be removed below 500°C, which indicates that there is little formation of hard-coke. Most of the coke may still have a relatively high H/C ratio and would be non-graphitic in nature.

To investigate the evolution of the formation of coke along the reactor, we have conducted TPO measurements of preheated samples of catalysts A and D taken from four different positions in the reactor: top of the first reactor, and top, center and bottom of the second reactor. As shown in Fig. 5 for sample A, the amount of deposits at the top of the first reactor is very low. This was the only sample that exhibited very small oxidation peaks at temperatures which would correspond to graphitic carbon. However, the rest of the samples showed that as the amount of coke deposits increased along the reactor, the nature of these deposits did not change significantly since they showed essentially the same oxidation behavior. As mentioned above, catalyst D formed very small amounts of deposits that could not be eliminated by the preheating in He. As shown in Fig. 6, in this case again, the only sample that exhibited a somewhat more refractory coke was that from the inlet of the first reactor. Other than that, all the coke deposits were very similar.

The BET area and pore size distribution measurements were conducted on fresh and aged samples after

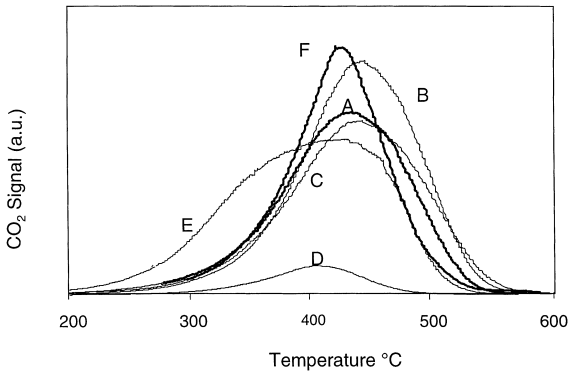

Fig. 4. Temperature-programmed oxidation profiles for the different catalysts aged in the bottom of the second reactor.

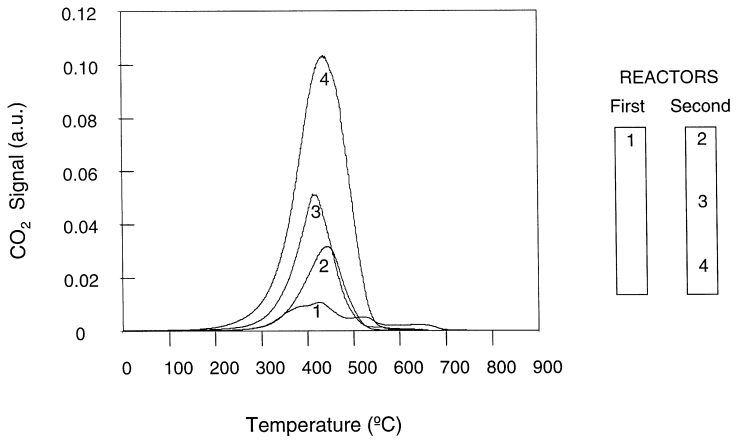

Fig. 5. Temperature-programmed oxidation profiles for different samples of catalyst A aged at indicated locations along the two reactors.

toluene extraction and drying under vacuum. A typical pore size distribution for fresh and spent catalysts is shown in Fig. 7 for catalyst E. As expected, the size of the main peak was significantly smaller for the aged catalyst. The aged samples from the top of the first reactor showed a more drastic reduction in size, consistent with a much larger accumulation of metals at this location. On the other hand, the samples from the bottom of the second reactor, which exhibited less metals and much more coke exhibited the appearance of microporosity, which is typical of carbonaceous deposits, and a lower decrease in the size of the main peak, indicating a lower degree of pore blocking. Table 5 summarizes the distribution of surface area in three different pore size ranges (<60, 60–100 and >100 Å). In all cases, the microporosity increases in the aged catalysts. The porosity in the range 60–100 Å increased or decreased upon aging depending on the catalyst. For those with high initial porosity in this range it decreased, for those with low porosity in this range it increased. This trend indicates that some of the pores in this region are blocked under reaction, but at the same time, larger pores may be partially blocked, resulting in increased porosity in this range for those catalysts with high porosity in the larger pore range. It can be expected that diffusional limitations

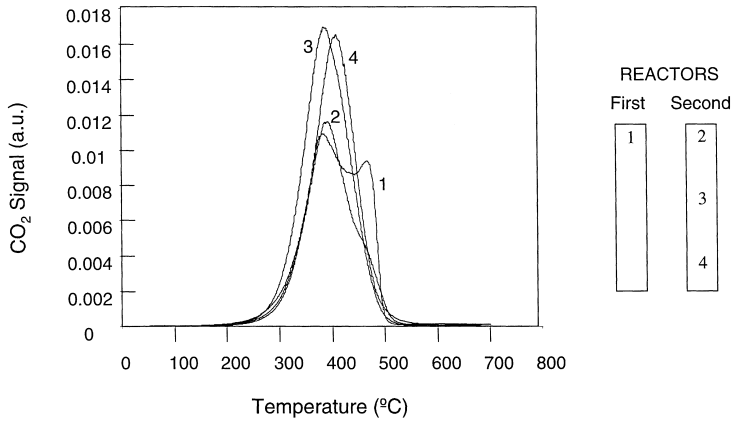

Fig. 6. Temperature-programmed oxidation profiles for different samples of catalyst D aged at indicated locations along the two reactors.

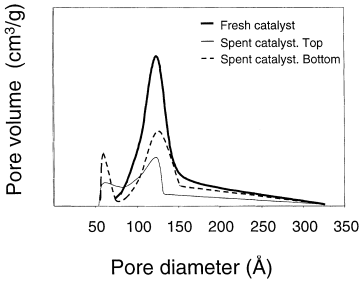

Fig. 7. Pore size distribution for catalyst E. Fresh catalyst (heavy solid line), catalyst aged at the top of the first reactor (light solid line), catalyst aged at the bottom of the second reactor (dashed line).

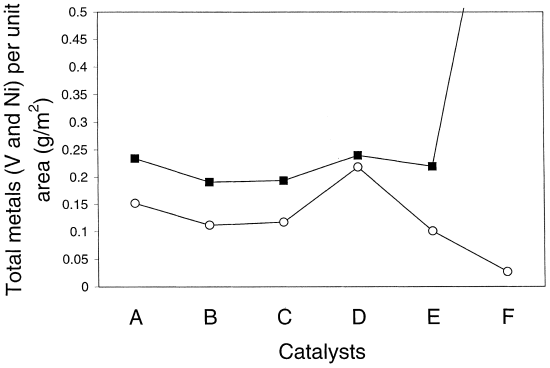

Fig. 8. Total metals (V and Ni) retained expressed per unit area. Open circles: metals retained per total BET area. Solid squares: metals retained per area in the pore size range above 100 Å.

and pore blockage will be less pronounced in those pores larger than 100 Å. Therefore, it is interesting to compare the total amount of metals retained based both on the overall surface area and on the area in the range >100 Å. This comparison is made in Fig. 8 which shows that the ratio of metals/area in the pores above 100 Å is almost a constant for all the catalysts except for sample F, which has very little area in that pore size range. By contrast, when the retained metals are referred to the total surface area, the value for sample F is very small and those for the other samples is not as constant as in the previous comparison, indicating that the smaller pores are rapidly blocked and are not able to retain a significant amount of metals and the activity of all catalysts is essentially proportional to the surface area with pore size greater than 100 Å. The slight deviation from the constant metals/area (>100 Å) ratio exhibited by samples B and C can be traced to the larger pellet size of sample B and the lower Mo–Ni loading of catalyst C. The smallness of this deviation indicate that these parameters have only a minor effect compared to surface area.

The deactivation of fresh catalysts was investigated in the trickle-bed laboratory reactor. As illustrated in Fig. 9, the hydrodemetallation activity rapidly drops during the first 30 h on stream, but then it stabilizes and starts a much slower deactivation process, as previously described in the literature [2]. The carbon accumulation measured after a 60 h reaction period, followed by toluene extraction and vacuum drying, was only 0.8 wt.% C. To compare the aged samples with fresh samples, we wanted to eliminate the initial short-term activity. So, the activity data reported below correspond to those obtained after an initial period

Table 5
Surface area distribution (m^2/g) in different pore size ranges (Å) for the fresh and aged catalysts

Catalyst	Fresh catalysts			Aged catalyst			Aged catalyst		
				Top of first reactor			Bottom of second reactor		
	0–60	60–100	100+	0–60	60–100	100+	0–60	60–100	100+
A	32	80	208	33	52	8	89	11	101
B	16	94	156	32	38	75	26	24	86
C	14	90	160	45	39	85	75	47	98
D	4	9	133	69	33	30	63	14	50
E	9	134	122	35	45	22	74	18	27
F	118	201	10	89	71	6	165	42	5

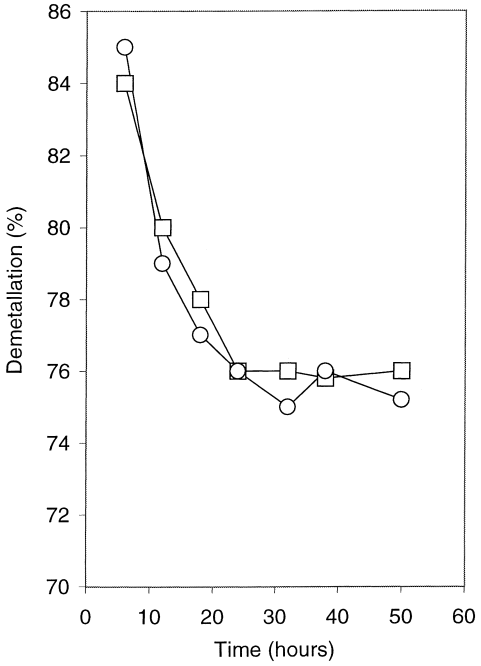

Fig. 9. Demetallation activity expressed as percent of metals retained as a function of time at the beginning of the run in the laboratory reactor at 350°C, LHSV of 2, 1500 psia. Ni retention (circles) V retention (squares).

of 40 h on stream, at which time a stable activity level was achieved. Table 6 summarizes the Ni and V conversions obtained in the laboratory reactor on fresh and aged samples of catalysts A, D and F. As mentioned above, catalyst A has high surface area and large pore size, catalyst D large pore size, but lower surface area, and catalyst F high surface area, but small pore size.

Table 6
Quality of product obtained in the laboratory reactor at 350°C and at a LHSV of 2 on fresh and spent catalysts

	V conversion (%)	Ni conversion (%)
A (fresh)	75.7	76.1
D (fresh)	69.3	77.7
F (fresh)	45.7	50
$A_{(T)}$	19.3	23.1
$D_{(T)}$	47.1	60
$F_{(T)}$	2.8	38.5
$A_{(B)}$	62.1	63
$D_{(B)}$	62.8	67
$F_{(B)}$	6.4	21.5

The activity of the fresh catalysts obtained on the laboratory reactor correlates very well with the total accumulation of metals observed during the long run in the industrial reactor. Accordingly, catalyst A exhibited higher activity than catalyst D and much higher than catalyst F. The residual activity of the aged catalysts was very different between the samples aged on the top of the first reactor and those aged in the bottom of the second reactor. For all three catalysts, the former were much more deactivated than the latter. On the top of the first reactor, both the least active catalyst F and the most active catalyst A were almost completely deactivated, while the intermediate catalyst D retained some residual activity. On the other hand, in the bottom of the second reactor, both catalysts A and D retained high activity while the small-pore catalyst F was completely deactivated.

4. Discussion

The main cause of catalyst deactivation in the hydrotreating of deasphalted vacuum bottoms is the deposition of metals, but some contribution towards deactivation comes from the accumulation of heavy hydrocarbon molecules in the interior of the pore structure, particularly in the second reactor. The comparative aging process studied in this work under the same reaction conditions indicates that the pore size, surface area, and pellet size may result in different deactivation patterns. Most of the differences in deactivation are due to the different diffusion patterns in the various samples investigated. Recent investigations of the deactivation of hydrotreating catalysts have shown that the overall demetallation activity is much more affected by parameters associated with effective diffusivity than with those associated with the rate constant [3]. This is particularly important when the size of the diffusing molecules becomes of the same order as the pore size. In this range, the effective diffusivity is greatly reduced as the pore size decreases [4]. Asphaltenes have the tendency to agglomerate and form clusters, which may have molecular weights above 2000 [5]. Resines have similar structures but they do not seem to form clusters. In any case, these molecules have sizes that may range from 25 to 150 Å, with the majority around 50 Å [6]. Therefore, it is expected that the smaller pores in the catalyst will be

quickly plugged as in the case of catalyst F, and the long-term catalyst activity will be only related to the surface area corresponding to the largest pores, i.e. >100 Å.

To interpret the observed metal deposition patterns on the different series one needs to take into consideration both, the molecular size as well as the reactivity of the different compounds present in the feed. Each of the deposition profiles observed in the catalyst series can be classified in one of the following categories, previously reported in the literature:

4.1. M-shaped profiles

These profiles have been previously observed for the deposition of vanadium and nickel on different catalysts [7–10]. The shape of these profiles is due to the nature of the demetallation reaction, which occurs though a consecutive mechanism. As proposed by Quann et al. [2], this mechanism starts with the formation of a metal-depositing intermediate resulting from the interaction of the metalloporphyrins with the surface, and it is then followed by the accumulation of metals. Therefore, as the metalloporphyrin penetrates the pore, it starts a conversion process that eventually ends in the deposition of the metal. Accordingly, the position of the maxima inside the pores depends not only on the reactivity of the surface and the metalloporphyrin, but also on the diffusion parameters. Therefore, it varies with temperature, pressure, pore structure and position in the reactor. Tamm et al. [11] noted that the maxima in the M-shaped profiles observed for the deposition of metals shifted towards the pellet's edge as a function of position in an industrial packed-bed reactor. The reason for this shift is that the deposition does not occur from the compounds originally present in the feed, but rather through an intermediate that is formed either through the pore or along the reactor. Therefore, while at the reactor inlet it may need to penetrate in the pore before it is formed, along the reactor is readily available near the pore mouth.

4.2. U-shaped profiles

These profiles exhibit maxima at the pellet's edges and have been reported in the literature for catalysts located at the reactor outlet, and particularly for the deposition of vanadium [11–13]. U-shaped profiles occur more readily with vanadium than with Ni because the intrinsic reactivity of vanadium porphyrins is normally higher than that of the Ni porphyrins.

4.3. Uniform distribution

This profile has been frequently reported in the literature [8,14]. In this case, the rate of diffusion is high and the rate of deposition slow enough to prevent inhomogeneous accumulation inside the pore. Therefore, this profile is typical of Ni deposition, which exhibits low reactivity and catalysts with large pores.

4.4. Maximum in the center

These profiles have previously been reported by Jansen et al. [15], who used V-porphyrins diluted in *o*-xylene in a catalyst with large pores (>500 Å). They explain this profile by the low resistance to diffusional transport and by the sequential deposition mechanism described above. In this case, not only the molecules need to be converted to react, but they can easily penetrate inside the pellet.

The overall trends observed in the catalyst series reported in this contribution can be very well explained in terms of the competition between the diffusion and adsorption/reactivity parameters. As the pore size increases the diffusional limitations become less important, and as mentioned above V-compounds are more easily adsorbed than Ni-compounds. Therefore, in general the Ni-compounds exhibit a deeper penetration into the pellet than the V-compounds as a result of their lower reactivity. When the pore size becomes too small, as in the case of catalysts E and F, the diffusional resistance becomes dominant and both Ni and V are deposited preferentially in the external part of the pellet. As the pore size increases to about 100 Å, a clear difference in profiles is observed for Ni and V. Catalysts A, with pore size 126 Å, and catalyst B, with 98.6 Å, clearly show the difference in reactivity. While for Ni the profiles are homogeneous due to a higher diffusion rate than adsorption rate, for V the diffusion rate is still too slow for the more

reactive V-compounds, so U-shaped profiles result. Finally, when the pores are very large neither Ni- nor V-compounds are subject to strong diffusional limitations and both profiles become homogeneous. This is the case for catalysts C (pore size 136 Å) and D (pore size 233 Å). Interestingly, despite the homogeneous profile presented by catalyst C for both V and Ni, the total amount of V retained is much larger than that of Ni. This difference can be ascribed to the very low Ni–Mo active metal content present on the fresh catalyst. It is apparent that the lower activity of this catalyst has a more pronounced effect on the adsorption of the Ni-compounds, which are harder to activate than the V-compounds. On the other hand, despite the low diffusional limitations exhibited by catalyst D, due to its large pore size, the total amount of metal retention is relatively low. This is due to the much lower overall surface area of this catalyst, compared to catalyst A, which has smaller pores, but larger surface area. In this case, however, the residual activity after the 240-day run was almost zero, while catalyst A, retained a high activity. Catalyst A, therefore, is a more active catalyst, but with shorter life.

According to the present comparison we may infer that the ideal catalyst should have a combination of:

1. high initial activity, given by the active-metal loading and surface area in the proper pore range (e.g. >100 Å),
2. homogeneous distribution of metal deposition to assure a uniform utilization of the catalyst; this is achieved by increasing pore size and reducing pellet size, which minimizes the diffusional limitations.

The latter condition will also impact catalyst life, since a catalyst with small pore size will quickly deactivate. As illustrated for the case of catalyst F, a large surface area with small pore size results in a catalyst of poor performance. At the other extreme, a very large pore would result in relatively low surface area. This situation would not be optimal either, since despite a long catalyst life, the overall catalyst activity could be too low.

A similar analysis of the deactivation of this type of catalysts has been done by Dadyburjor and Raje [16], who investigated the relative importance of two types of deactivation mechanisms, site suppression and pore choking. In a quantitative study of the kinetic and mass-transfer parameters of coal–liquid Ni–Mo hydrotreatment catalysts, they compared the deactivation by suppression of sites and by choking of catalyst pores during the deposition of coke and metals. Their results showed that the deactivation by pore choking is much more important than that by site suppression, and only after long periods of deactivation, does the site suppression begins to decline. In our case, regarding the deactivation by coke formation, this only becomes important near the outlet of the second reactor and even at that point there is no formation of hard-coke, as demonstrated by the low-oxidation temperatures shown in the TPO experiments. Here again, the pore structure has an important effect on the nature of the carbonaceous deposits and its deactivating effects. The most interesting catalyst in this sense was catalyst D, which exhibited reversible deposition of carbonaceous species. This species can be removed by heating in inert atmosphere for a couple of hours and do not result in permanent deactivation of the catalyst. As shown in the laboratory reactor measurements, catalyst D showed a very low extent of deactivation, both on the top of the first reactor as well as at the outlet of the second reactor. Similarly, catalyst A, with a large pore size presented little deactivation in the second reactor, where coke deposition occurs, but was completely deactivated on the top of the first reactor as a result of its high activity for metal deposition. Catalyst B, with the largest pellet size, exhibited the greatest amount of carbon deposits, not only in the second reactor, but remarkably at the top of the first reactor. The excessive coke deposition in the first reactor could be explained in terms of a series mechanism for coke formation similar to that described for the demetallation. Accordingly, the coke formation would occur after partial transformation of the molecules and formation of a coke precursor, which can either form along the reactor, or in the case of large pellet along the pore.

The TPO analysis of the carbonaceous deposits obtained along the reactor for catalysts A and D helps to shed some light on the coking mechanism. In the case of catalyst A, the amount of carbonaceous deposits, which cannot be eliminated by heating in inert atmosphere gradually increases along the reactor. This gradual increase can be explained in terms of the gradual formation of coke precursors, as mentioned

above. On the other hand, catalyst D, for which most of the carbonaceous deposits were easily eliminated by heating, the amount of coke deposits does not vary significantly along the reactor. This difference may indicate that in catalyst D, which has much larger pores than catalyst A, the residence time of the molecules inside the pores is too short for the formation of the coke precursors.

5. Conclusions

The deactivation of hydrotreating catalysts for deasphalted vacuum bottoms depends on several factors, which include: the chemical characteristics of the feed, the pore structure, active metal loading, surface area and pellet size of the catalyst, as well as the position along the packed-bed reactor. In the upper part of the first reactor, the deactivation by metals is dominant. The distribution of metals inside the catalyst pellet depends on a competition between diffusion and activity for adsorption/deposition. The former is determined by pore and pellet sizes, the latter by surface area and active metal loading. When the activity is too high in comparison to the diffusion rate, the deposition occurs preferentially at the pore mouth. This leads to pore blockage and rapid deactivation. Due to a lower intrinsic activity of the corresponding porphyrins, Ni tends to distribute more uniformly throughout the pellet than V.

Coke formation only occurs to a low extent and it is only significant at the end of the second reactor. Even at this point the coke formed is not of the ‘hard’ type and can be removed by oxidation at moderate temperatures. In some cases, such as in the catalysts of the largest pore size, it can be removed by heating in inert atmosphere.

Acknowledgements

We want to thank Ecopetrol-ICP for financial support and the Energy Institute of the Americas for starting the research collaboration.

References

[1] R.A. Dean, E.V. Whitehead, Proc. 6th World Petrol. Congress, paper V-9, 1963.
[2] R.J. Quann, R.A. Ware, C. Hung, J. Wei, Adv. Chem. Eng. 14 (1988) 95.
[3] T. Takatsuka, S. Higashino, S. Hirohama, Y. Wada, R. Kajiyama, Proc. 210th National Meeting American Chemical Society, Chicago, 1995.
[4] Y. Chen, M. Tsai, Can. J. Chem. Eng. 72 (1994) 854.
[5] R.L. Griffin, W.C. Simpson, T.K. Miles, ACS Proc. Div. Petrol. Chem. 3 (1958) A13.
[6] E. Ruckenstein, M.C. Tsai, AIChE. J. 27 (1978) 1104.
[7] N. Todo, T. Kabe, K. Ogawa, M. Kurita, T. Sato, K. Sihmada, Y. Kuriki, T. Oshima, T. Takematsu, Kotera. Kogyo Kagaku Zasshi 74 (1971) 563.
[8] M. Sato, N. Takayama, S. Kurita, T. Kwan, Nippon Kagaku Zasshi 92 (1971) 834.
[9] M. Inoguchi, H. Kagaya, K. Diago, S. Sakurada, Y. Satomi, K. Inaba, K. Tate, R. Nishiyama, S. Onishi, T. Nagal, Bull. Jpn. Petrol. Inst. 13 (1971) 153.
[10] M.F. Oxenreiter, C.G. Frye, G.B. Hoekstra, J.M. Sroka, Jpn. Petrol. Inst. 30 (1972).
[11] P.W. Tamm, F.H. Harnsberger, A.G. y Bridge, Ind. Eng. Chem. Process Des. Dev. 20 (1981) 262.
[12] P.R. Fozard, J.W. McMillan, P. Zeuthen, J. Catal. 152 (1995) 103–115.
[13] J. Bartholdy, P. Hannerup, Hidrodemetallization in resid hydroprocessing. Stud. Surf. Sci. Catal. 68 (1991) 273; Catalyst Deactivation, Elsevier, Amsterdam, 1991.
[14] H.D. Simpson, Surf. Sci. Catal. 68 (1991) 265; Catalyst Deactivation, Elsevier, Amsterdam, 1991.
[15] J.P. Janseen, R.M. Deugd, A.D. Langeveld, S.T. Sie, J.A. Moulijn, Surf. Sci. Catal. 111 (1997) 283; Catalyst Deactivation, Elsevier, Amsterdam, 1997.
[16] D.B. Dadyburjor, A.P. Raje, J. Catal. 145 (1994) 16.